Unimolecular Rate Constants for HX or DX Elimination (X = F, Cl) from Chemically Activated $CF_3CH_2CH_2Cl$, $C_2H_5CH_2Cl$, and $C_2D_5CH_2Cl$: Threshold Energies for HF and HCl Elimination

J. D. Ferguson,[†] N. L. Johnson,[‡] P. M. Kekenes-Huskey,[||] W. C. Everett,[||] G. L. Heard,[||] D. W. Setser,[§] and B. E. Holmes*,[||]

Lyon College, 2300 Highland Road, Batesville, Arkansas 72503-2317, and University of North Carolina at Asheville, One University Heights, Asheville, North Carolina 28804-8511

Received: November 30, 2004; In Final Form: March 8, 2005

Vibrationally activated $CF_3CH_2CH_2Cl$ molecules were prepared with 94 kcal mol^{-1} of vibrational energy by the combination of CF_3CH_2 and CH_2Cl radicals and with 101 kcal mol^{-1} of energy by the combination of CF_3 and CH_2CH_2Cl radicals at room temperature. The unimolecular rate constants for elimination of HCl from $CF_3CH_2CH_2Cl$ were 1.2×10^7 and 0.24×10^7 s^{-1} with 101 and 94 kcal mol^{-1}, respectively. The product branching ratio, k_{HCl}/k_{HF}, was 80 ± 25. Activated $CH_3CH_2CH_2Cl$ and $CD_3CD_2CH_2Cl$ molecules with 90 kcal mol^{-1} of energy were prepared by recombination of C_2H_5 (or C_2D_5) radicals with CH_2Cl radicals. The unimolecular rate constant for HCl elimination was 8.7×10^7 s^{-1}, and the kinetic isotope effect was 4.0. Unified transition-state models obtained from density-functional theory calculations, with treatment of torsions as hindered internal rotors for the molecules and the transition states, were employed in the calculation of the RRKM rate constants for $CF_3CH_2CH_2Cl$ and $CH_3CH_2CH_2Cl$. Fitting the calculated rate constants from RRKM theory to the experimental values provided threshold energies, E_0, of 58 and 71 kcal mol^{-1} for the elimination of HCl or HF, respectively, from $CF_3CH_2CH_2Cl$ and 54 kcal mol^{-1} for HCl elimination from $CH_3CH_2CH_2Cl$. Using the hindered-rotor model, threshold energies for HF elimination also were reassigned from previously published chemical activation data for $CF_3CH_2CH_3$, $CF_3CH_2CF_3$, $CH_3CH_2CH_2F$, CH_3CHFCH_3, and $CH_3CF_2CH_3$. In an appendix, the method used to assign threshold energies was tested and verified using the combined thermal and chemical activation data for C_2H_5Cl, C_2H_5F, and CH_3CF_3.

Introduction

Fluoropropane and chlorofluoropropane molecules have some applications that would benefit from an understanding of their unimolecular decomposition reactions. Conventional thermal pyrolysis data often are compromised by competing free-radical reactions, hence few studies have been made. Our laboratory[1−4] has initiated a program to assign threshold energies and transition-state models to these reactions based upon chemical activation studies. In the present work, we have investigated the $CF_3CH_2CH_2Cl$ molecule at 94 and 101 kcal mol^{-1} and $C_2H_5CH_2Cl$ and $C_2D_5CH_2Cl$ molecules at 90 kcal mol^{-1}. Measurement of the ratio of the olefin product from HCl and HF elimination versus the collisionally stabilized product as a function of pressure at room temperature gives the experimental unimolecular rate constant. The main goal of the current work is to use the experimental results together with density-functional theory (DFT) computations of reactant and transition-state structures and statistical unimolecular rate theory (RRKM) calculations of rate constants to assign threshold energies, E_0, of these reactions. In addition, the published chemical activation data for $CF_3CH_2CH_3$, $CF_3CH_2CF_3$, $CH_3CH_2CH_2F$, CD_3CHFCH_3, and $CH_3CF_2CH_3$ are used to assign threshold energies for HF elimination from these molecules systematically.

Early studies of chemically activated haloethanes and halopropanes[5−10] using a unified, but empirical, formulation of a transition-state model for HX (X = F, Cl, Br) elimination demonstrated good agreement between the RRKM calculations, which were based upon threshold energies and preexponential factors from thermal activation, and chemical activation rate constants that were measured at 90−95 kcal mol^{-1}. These studies[5−10] provided examples that supported the validity of the statistical treatment of unimolecular reactions.[11] With the availability of electronic structure calculations, transition-state structures for HX elimination from fluorochloro ethanes and propanes can now be calculated.[12−14] These structures are rather insensitive to the nature of the calculation and basis sets. The inference is that the moments of inertia and vibrational frequencies of these transition states should be realistic or at least subject to systematic testing. However, the values calculated for the threshold energy change with the nature of the calculation and with the basis set.[13] Improved knowledge of the thermochemistry for the haloethanes and the radicals together with a better definition of the transition states invites a more critical comparison between the thermal and chemical activation data. In addition to improving the model for the transition state, more rigorous treatment of the torsional motions, which are actually hindered internal rotations, for the haloethane and halopropane molecules is needed. In the present application of the RRKM theory, we have (i) adopted transition-state models obtained from DFT and (ii) calculated sums of states, density

* Corresponding author. E-mail: bholmes@unca.edu.
[†] Lyon College.
[‡] Johnson C. Smith University, Charlotte, North Carolina.
[§] Kansas State University, Manhattan, Kansas.
[||] University of North Carolina at Asheville.

10.1021/jp040735g CCC: $30.25
Published on Web 04/30/2005

of states, and partition functions for torsional motions as hindered internal rotors. The calculations still employ the harmonic oscillator approximation for the sums and densities of states for the vibrational modes in the evaluation of the RRKM rate constants. Reliable thermal and chemical activation data have been reported for C_2H_5Cl, C_2H_5F, and CH_3CF_3. Therefore, in an appendix we have reexamined the thermal and chemical activation results based on the calculated transition-state models. Although differing in a few details from the original interpretations, the agreement between the model calculations and the thermal and chemical activation data is satisfactory for a common value of the threshold energy. The analysis for C_2H_5F, C_2H_5Cl, and CH_3CF_3 provides justification for application of the same methodology to chemical activation data of halopropanes to obtain the threshold energies reported in this and subsequent papers.

An important variable in converting chemical activation data to unimolecular rate constants is the model for collisional deactivation. In the present experiments, the bath gases are small organic molecules containing iodine atoms. Extensive studies of collisional deactivation of haloethanes at room temperature[15−18] have shown that such collision partners are efficient with removal of 6−8 kcal mol^{-1} from the excited molecule per collision. For such bath gases, adjustment of the apparent rate constant measured at high pressure with cascade deactivation to the unit deactivation rate constant is minimal. However, selection of the best collision diameters for calculation of the collision rate constant ($z_{A,M} = \pi d^2_{A,M}(8kT/\pi\mu_{A,M})^{1/2}\Omega^{2,2*}$) directly affects the magnitude of the chemical activation rate constant. We have adopted the collisional diameters recommended by Hippler et al.[19] and Mourits and Rummens.[20]

The half-width of the thermal distributions[8] for the initially formed $CF_3CH_2CH_2Cl$ or $C_2H_5CH_2Cl$ molecules at 298 K is 3.5−4.5 kcal mol^{-1}. In principle, the RRKM rate constant, k_E, should be averaged over the distribution to obtain $\langle k_E \rangle$, which is equivalent to the limiting high-pressure experimental rate constant. However, the value of $k_{\langle E \rangle}$ is the same as $\langle k_E \rangle$ to within 10−15%. In fact, the uncertainty in the ΔH°_f of the radicals and molecules introduces an uncertainty in $\langle E \rangle$ that is more serious than the difference between $k_{\langle E \rangle}$ and $\langle k_E \rangle$, and we have employed $k_{\langle E \rangle}$ for comparison with the experimental rate constants measured at room temperature.

With the calculation of vibrational frequencies and zero-point energies and the assignment of E_0 for $CH_3CH_2CH_2Cl$, the calculation of the intermolecular kinetic isotope effect for $CD_3CD_2CH_2Cl$ has no adjustable parameters. Thus, the isotope effect provides a consistency check for the data and for the transition-state models. The isotope effect depends on $E_{0,H} - E_{0,D}$ and the statistical secondary kinetic isotope effect; the latter is about 1.3 per H/D substitution.[5,13,21] If the E_0 does not change, then the reduction in k_E upon replacement of CH_3 by CF_3 also can be viewed as a statistical secondary kinetic isotope effect, which is about a factor of 1.7 per F atom.[22] Depending on the position in the molecule, substitution of F for H or Cl can change the threshold energy. Electronic structure calculations of threshold energies for HX elimination for a series of molecules frequently give the correct trends for changes in E_0 but not necessarily the correct magnitude for substituents in the α and β positions.[3b,12−14] For this reason, as well as the practical need, experimental assignment of threshold energies for fluoropropanes and fluorochloropropanes is desirable.

Experimental Methods

The desired radicals for generation of $CF_3CH_2CH_2Cl$ were produced by photolysis of iodine-containing compounds with a high-pressure Oriel 6137 mercury lamp. A 313 nm band-pass filter was used for photolysis of CH_2ClCH_2I to augment the short-wavelength cutoff of Pyrex glass. Pyrex glass vessels with volumes ranging from 14.85 to 3505.6 cm^3 containing a total of 2.45 μmol of reactants in 1:5 CF_3I/CH_2ClCH_2I were photolyzed to generate CF_3 and C_2H_4Cl radicals, which recombine to form $CF_3CH_2CH_2Cl$. In other experiments, 0.818−3.27 μmol in 1:3 CH_2ClI/CF_3CH_2I was photolyzed for 3−10 min at room temperature to form $CF_3CH_2CH_2Cl$ at a lower energy. Small amounts of solid Hg_2I_2 were added to the vessels to scavenge iodine atoms and I_2. The utility of the Hg_2I_2 in the photolysis of RI systems has been discussed and tested.[23] All samples were prepared on a grease-free vacuum line using an MKS 270 electronic manometer for the measurement of pressure. Products were identified and measured using a Shimadzu GC-14A gas chromatograph equipped with a $^1/_8$ in. × 14 ft Porapak T column and a flame-ionization detector. The operating conditions for the gc column were an initial temperature of 110 °C with immediate temperature programming at a rate of 1 °C/min to a maximum temperature of 170 °C. Retention times (in min) were as follows: C_2F_6 and CF_3H (2.2), C_2H_4 (2.4), $CF_3CH{=}CH_2$ (7.4), $CF_3CH_2CH_3$ (8.1), $CH_2{=}CHCl$ (10.4), CF_3I (10.6), $CF_3CH_2CH_2CF_3$ (23.8), $CF_2{=}CHCH_2Cl$ (33), $CF_3CH_2CH_2Cl$ (42), CF_3CH_2I (50), CH_2ClCH_2Cl (63), CH_2ClI (75), and CH_2ClCH_2I (127).

Products were identified by comparison of GC retention times with authentic samples and verified with a Hewlett-Packard 5890 series II gas chromatograph with a 100 m × 0.25 mm RTX-200 column coupled with a 5971 Hewlett-Packard series mass selective detector. The $CF_2{=}CHCH_2Cl$ peak could not be directly identified because a commercial sample of this compound was not available. Furthermore, the amount of $CF_2{=}CHCH_2Cl$ was small, and it was difficult to obtain a complete mass spectrum. The small peak eluted just before the $CF_3CH_2CH_2Cl$ peak (containing $m/e = 51$, corresponding to HCF_2^+, and 77, corresponding to $CF_2{=}CHCH_2^+$) was assigned to $CF_2{=}CHCH_2Cl$. Because a commercial sample of $CF_2{=}CHCH_2Cl$ was not available, the response for the gas chromatograph was assumed to be the same as for $CH_2{=}CHCH_2Cl$.

Chemically activated $C_2H_5CH_2Cl$ ($C_2D_5CH_2Cl$) molecules were prepared by the combination of CH_3CH_2 (CD_3CD_2) and CH_2Cl radicals. Reaction mixtures containing 18.54 μmol of CH_3CH_2I (CD_3CD_2I) and 1.234 μmol of CH_2ClI, which were prepared as described above, were photolyzed for 1 to 3 min, depending on the size of the vessel. The photolysis vessels were Pyrex glass vessels ranging in volume from 7.452 to 183.1 cm^3, which contained a small amount of solid Hg_2I_2 (and Hg). Following photolysis, reaction mixtures were analyzed using a Shimadzu gas chromatograph (GC-14A) equipped with a 0.53 mm × 105 m RTX-VGC column and a flame-ionization detector. Peak areas were integrated by a Shimadzu C-R5A Chromatopac integrator. Products were identified by comparison of retention times with authentic samples on the GC-14A and by analysis using a Shimadzu QP 5000 GC-MS, which had a 0.25 mm × 60 m RTX-VMS capillary column. Typical retention times (min) on the GC-14A were C_3H_6 (9.0), $C_2H_5CH_2Cl$ (24.5), CH_3CH_2I (33), and CH_2lCl (43); retention times for the deuterated analogues were slightly shorter. The relative response of a flame-ionization detector for propene and 1-chloropropane was measured as 1.06 ± 0.03 upon the basis of four trials of three different mixtures of propene and 1-chloropropane containing excess C_2H_5I to aid the transport of the mixture to the injection system of the gas chromatograph.

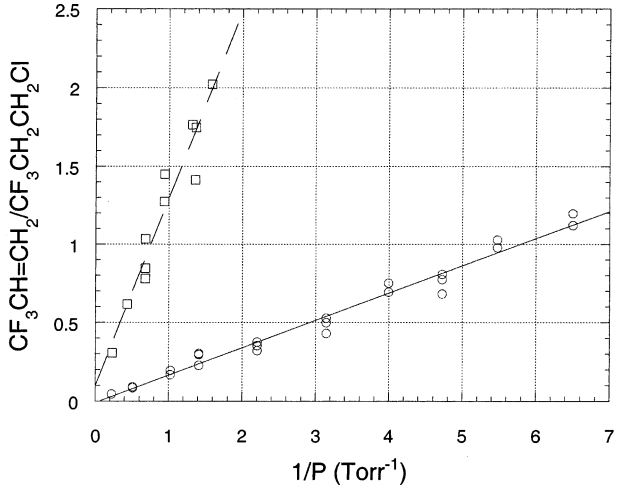

Figure 1. Plot of $[CF_3CH{=}CH_2]/[CF_3CH_2CH_2Cl]$ vs reciprocal pressure for the elimination of HCl from $CF_3CH_2CH_2Cl$ with 94 kcal mol^{-1} (○) and 101 kcal mol^{-1} (□) of internal energy. The slope is 0.81 ± 0.12 Torr, the intercept is 0.098, and the correlation coefficient is 0.96 for the data at 101 kcal mol^{-1}; the same values are 0.174 ± 0.005 Torr, −0.01, and 0.99, respectively, for $CF_3CH_2CH_2Cl$ with 94 kcal mol^{-1} of energy.

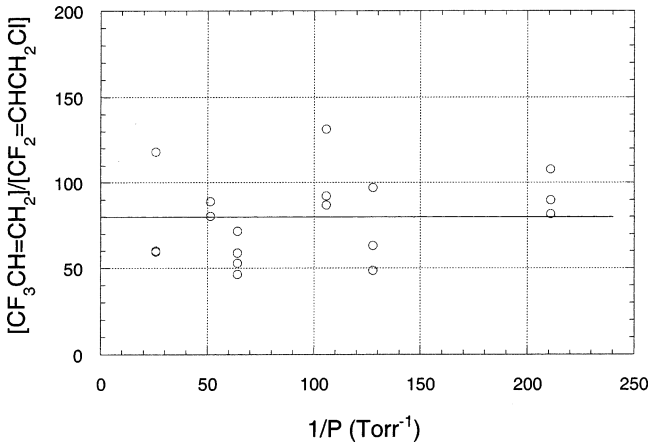

Figure 2. Plot of $[CF_3CH{=}CH_2]/[CF_2{=}CHCH_2Cl]$ versus reciprocal pressure for chemically activated $CF_3CH_2CH_2Cl$ with 94 kcal mol^{-1} of energy.

Experimental Results

A. Rate Constants for $CF_3CH_2CH_2Cl$, n-C_3H_7Cl, and $C_2D_5CH_2Cl$. The unimolecular rate constants (k_{HCl}) for elimination of HCl from $CF_3CH_2CH_2Cl$ were determined from plots of $CF_3CF{=}CH_2(D_1)/CF_3CH_2CH_2Cl(S)$ versus inverse pressure; see Figure 1.

$$CF_3CH_2CH_2Cl \rightarrow CF_3CH{=}CH_2\,(D_1) + HCl \quad (1a)$$

$$\rightarrow CF_2{=}CHCH_2Cl\,(D_2) + HF \quad (1b)$$

$$CF_3CH_2CH_2Cl + M \rightarrow CF_3CH_2CH_2Cl\,(S) \quad (1c)$$

The plot of the D_1/S ratio versus inverse pressure for $CF_3CH_2CH_2Cl$ molecules formed with 94 kcal mol^{-1} had a slope of 0.174 ± 0.005 Torr. The data span the D_1/S range from 0.1 to 1.1, and the high-pressure intercept is zero. The $CF_3CH_2I + CH_2ClI$ photolysis system was very clean, and the major products were the ones shown in eq 1 plus $CF_3CH_2CH_2CF_3$, $CH_2{=}CHCl$, and small amounts of CH_2ClCH_2Cl. These results should be a reliable measure of the average rate constant for HCl elimination at 94 kcal mol^{-1}.

The rate constant for HF elimination from $CF_3CH_2CH_2Cl$ is much smaller than for HCl elimination. Thus, the yield of $CF_2{=}CHCH_2Cl$ was small and difficult to measure. The ratios of the $CF_2{=}CHCH_2Cl$ and $CF_3CH{=}CH_2$ products from the CF_3CH_2I with CH_2ClI experiments are shown in Figure 2, and the average k_{HCl}/k_{HF} ratio is 80 ± 25.

The combination of CF_3 and CH_2CH_2Cl radicals was used to generate molecules with 101 kcal mol^{-1} of internal energy. Unfortunately, the reaction chemistry was far more complex than for the $CF_3CH_2 + CH_2Cl$ system. Typically, ~75% of the product yield consisted of three dominant products: $CH_2{=}CH_2$, CF_3Cl, and CH_2ClCH_2Cl; the CF_3H, $CF_3CH_2CH_3$, and $CF_3CH_2CH_2CF_3$ products were less important but still accounted for 15% of the yield. The remaining 10% of the yield consisted of C_2F_6, the products shown in reactions 1, and other products, which had very small yields that were not identified. Disproportionation reactions, which involve the transfer of a Cl from CH_2CH_2Cl, reactions 2 and 3, account for the three dominant products.

$$CF_3 + CH_2CH_2Cl \rightarrow CF_3Cl + CH_2{=}CH_2 \quad (2a)$$

$$\rightarrow CF_3H + CH_2{=}CHCl \quad (2b)$$

$$\rightarrow CF_3CH_2CH_2Cl \quad (2c)$$

$$2CH_2CH_2Cl \rightarrow CH_2{=}CH_2 + CH_2ClCH_2Cl \quad (3)$$

The addition of CF_3 radicals to ethene, reaction 4, and subsequent disproportionation−combination reactions,[24] reactions 5−7, account for the CF_3H, $CF_3CH_2CH_3$, and $CF_3CH_2CH_2CF_3$ yields.

$$CF_3 + CH_2{=}H_2 \rightarrow CF_3CH_2CH_2 \quad (4)$$

$$CF_3 + CF_3CH_2CH_2 \rightarrow CF_3H + CF_3CH{=}CH_2 \quad (5a)$$

$$\rightarrow CF_3CH_2CH_2CF_3 \quad (5b)$$

$$CF_3CH_2CH_2 + CH_2CH_2Cl \rightarrow CF_3CH_2CH_2Cl + CH_2{=}CH_2 \quad (6a)$$

$$\rightarrow CF_3CH{=}CH_2 + CH_3CH_2Cl \quad (6b)$$

$$2CF_3CH_2CH_2 \rightarrow CF_3CH_2CH_3 + CF_3CH{=}CH_2 \quad (7)$$

Several other possible radical combination reactions are not shown because those products were not detected. The $CF_3CH{=}CH_2$ produced by reactions 5a, 6b, and 7 is a serious complication because it augments the D_1 from reaction 1a. Reaction 6a produces additional $CF_3CH_2CH_2Cl$. We assume that reactions 6a and 6b occur at the same rate; thus, they will not seriously alter the slope of the line in Figure 1 because equal amounts of D_1 and S would be produced. Because the total yield of $CF_3CH_2CH_3$ was measured, it can be corrected for the $CF_3CH{=}CH_2$ from reaction 7 as an estimate for D_1. Finally, the $CF_3CH{=}CH_2$ from reaction 5a can be estimated using the disproportionation/combination rate constant ratio, k(5a)/k(5b), and the observed yield of $CF_3CH_2CH_2CF_3$ (reaction 5b). On the basis of eight trials of CF_3I photolysis in the presence of ethene, an average ratio of 0.2 ± 0.1 was measured for k(5a)/k(5b) in a vessel containing mercury and mercury iodides on the surface. The apparent k(5a)/k(5b) ratio had considerable scatter with some dependence on vessel size. In clean vessels using non-iodine-containing molecules as the radical sources, the disproportionation/combination rate constant ratio has been

TABLE 1: Summary of Experimental Rate Constants[a] for HCl or DCl Elimination

	$CF_3CH_2CH_2Cl$		$CH_3CH_2CH_2Cl$ or $CD_3CD_2CH_2Cl$	
system	Torr	s^{-1}	Torr	s^{-1}
$CF_3I + CH_2ClCH_2I$ mole ratio 1/5	0.81 ± 0.12	$1.2\ (\pm 0.2) \times 10^7$		
$CH_2ClI + CF_3CH_2I$ mole ratio 1/3	0.174 ± 0.005	$0.24\ (\pm 0.02) \times 10^7$		
$CH_2ClI + CH_3CH_2I$			5.41 ± 0.17	$8.69\ (\pm 0.27) \times 10^7$
$CH_2ClI + CD_3CD_2I$ mole ratio 1/15			1.36 ± 0.06	$2.17\ (\pm 0.10) \times 10^7$

[a] Conversion from Torr to s^{-1} was done using $k_a = N\pi d^2(8kT/\pi\mu)\Omega^{2,2}*$ with N being the concentration at the cited pressure for collision diameters and ϵ/k values of CF_3I (5.1 Å, 288 K), CH_2ClI (5.1 Å, 400 K), C_2H_5I (5.0 Å, 394 K), CH_2ClCH_2I (5.3 Å, 465 K), CF_3CH_2I (5.2 Å, 300 K), $CF_3C_2H_4Cl$ (5.3 Å, 410 K), and C_3H_7Cl (4.9 Å, 425 K).

reported to be 0.022.[23] Apparently, the presence of mercury and mercury iodides enhances disproportionation reactions on the surface of the vessels.

The plot of the adjusted D_1/S ratio versus inverse pressure for $CF_3CH_2CH_2Cl$ formed at the higher energy gives a line with a slope of 0.81 ± 0.12 Torr; see Figure 1. The data, which span the D/S range from 0.3 to 1.7, have a high pressure intercept of about 0.1, suggesting that the corrections did not fully compensate for all sources of $CF_3CH{=}CH_2$. The rate constant for molecules with 101 kcal mol^{-1} of energy is an upper limit; however, the results from the CH_2ClI/CF_2CH_2I system should be a reliable measure of the rate constant for HCl elimination at 94 kcal mol^{-1}.

Rate constants in pressure units were converted to s^{-1} using the collision diameters and ϵ/k values for CH_2ClCH_2I, CF_3CH_2-CH_2Cl, CF_3CH_2I, CH_2ClI, and CF_3I indicated in Table 1. These collision cross sections were taken from the tabulation given in refs 19 and 20. If the molecules were not in the list given by these references, then the computational method based upon critical data recommended by these authors was used to estimate the collision diameters and ϵ/k. The $\Omega^{2,2}*$ values, which are quite significant for these collision partners, were calculated using the equation given by Hippler, Troe, and Wendelken.[19] The rate constants for HCl elimination from $CF_3CH_2CH_2Cl$ are 1.2×10^7 and 0.24×10^7 s^{-1} at average energies of 101 and 94 kcal mol^{-1}, respectively.

The rate constants for HCl(DCl) elimination from C_3H_7Cl-($C_2D_5CH_2Cl$) were determined from D/S plots of propene/chloropropane versus reciprocal pressure from experiments with pressures ranging from 100 to 1.5 Torr; see Figure 3. More than 30 data points were collected for each molecule. Although some scatter develops in the D/S ratios for pressures below ~2.5 Torr, the data cover a wide range in D/S, and the intercepts are nearly zero; therefore, the results should be reliable. The rate constant for C_3H_7Cl is 5.41 ± 0.17 Torr, and that for C_2D_5-CH_2Cl is 1.36 ± 0.06 Torr. The kinetic isotope effect, without adjustment for the effect of mass on the collision frequency, is 3.97. These data were converted to rate constants in units of s^{-1} using the collision diameters and ϵ/k values specified in Table 1; the values are 8.69×10^7 and 2.17×10^7 s^{-1}, giving a kinetic isotope ratio of 4.0 ± 0.2. This rate constant for C_3H_7Cl is in agreement with an indirectly measured value[8] of $\sim 9 \times 10^7$ s^{-1}, which was for molecules formed from $CH_3 + CH_2CH_2Cl$ recombination at room temperature.

B. Rate Constants for $CH_3CH_2CF_3$, $CF_3CH_2CF_3$, CH_3CH_2-CH_2F, CD_3CHFCH_3, and $CH_3CF_2CH_3$. Rate constants for $CH_3CH_2CF_3$ and $CF_3CH_2CF_3$ have been reported recently from this laboratory.[1,2] Those values were adjusted to the collision diameters and ϵ/k values used in this work, and the values are listed in Table 3. The $CF_3CH_2CH_3$ molecules were generated

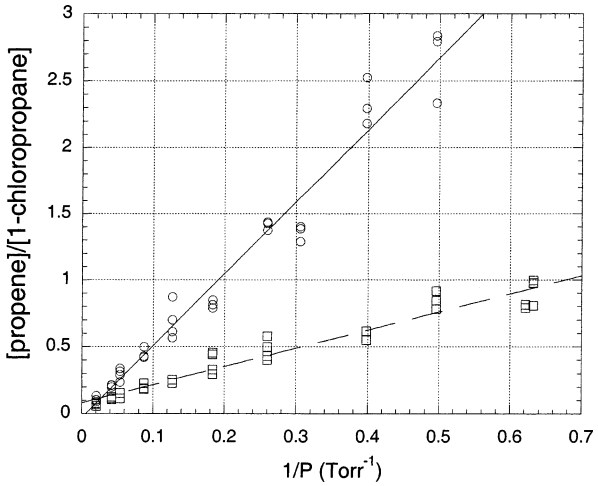

Figure 3. Plot (○) of $CH_3CH{=}CH_2/C_2H_5CH_2Cl$ vs reciprocal pressure for the elimination of HCl from $C_2H_5CH_2Cl$. The slope is 5.41 ± 0.17 with an intercept of -0.032, and the correlation coefficient is 0.97. The lower line is a plot (□) of $CD_3CD{=}CH_2/C_2D_5CH_2Cl$ vs reciprocal pressure for the elimination of DCl from $C_2D_5CH_2Cl$. The slope is 1.36 ± 0.06 with an intercept of 0.08, and the correlation coefficient is 0.95.

by recombination of CF_3 with C_2H_5 and CH_3 with CF_3CH_2, and rate constants are for 101 and 94 kcal mol^{-1} of energy.

The CD_3CHFCH_3 molecule was studied several years ago.[7] The main point at that time was to demonstrate that intramolecular vibrational relaxation (IVR) had occurred prior to HF or DF elimination. The intramolecular kinetic isotope effect, k_H/k_D, was normal, which showed that IVR was rapid relative to the time for reaction. The D/S versus inverse pressure plot[7] appears to be reliable, and we have converted the k_a in pressure units to s^{-1} using the collision diameters and ϵ/k values of choice for the current work. The data for this molecule seem to be a good test case for the transition-state model for HF and DF elimination.

Trotman-Dickenson and co-workers[9,10] investigated several chemically activated fluoroethanes and fluoropropanes. The D/S data for CH_2F recombining with CH_3CH_2 are extensive, and the rate constant for *n*-C_3H_7F from the 30 °C data is included in Table 3 (with adjustment for our choice of collision diameters). The $CH_2 + CH_3CHF_2$ reaction was used to prepare $CH_3CF_2CH_3$ and $CH_3CH_2CHF_2$ molecules. The $CH_3CH_2CHF_2$ molecule has both 1,1-HF and 1,2-HF elimination pathways, which were not resolved, and we will not attempt to interpret that unimolecular reaction. However, $CH_3CF_2CH_3$ can be treated by our methodology. Experimental data over the temperature range of −35 to 220 °C were collected using the internal standard method with photolysis of ketene plus added O_2 to suppress the free radical reactions. Although the internal

TABLE 2: Summary of Thermochemistry[a]

reaction ($R_1 + R_2$)	$\Delta H^\circ_{f298}(R_1)$	$\Delta H^\circ_{f298}(R_2)$	$\Delta H^\circ_{f298}(R_1R_2)$	$D_{298}(R_1-R_2)$	$\langle E(R_1-R_2)\rangle^h$
$C_2H_4Cl + CF_3$	22.2 ± 0.8^b	$-113.0 \pm 0.5^{c,e}$	-190 ± 2^d	99 ± 2	101 ± 2
$CF_3CH_2 + CH_2Cl$	-126.0 ± 1.6^e	28.0 ± 0.8^f	-190 ± 2^d	92 ± 2	94 ± 2
$C_2H_5 + CH_2Cl$	28.9 ± 0.5^g	28.0 ± 0.8^f	-31.5 ± 1^c	88.4 ± 1	90 ± 1

[a] All entries are in units of kcal mol^{-1}. [b] Reference 26. [c] Reference 27. [d] See the text. [e] Reference 28. [f] Reference 29. [g] Reference 30. [h] $\langle E_v(R_1 - R_2)\rangle = D_0(R_1 - R_2) + 3RT + \langle E_v(R_1)\rangle + \langle E_v(R_2\rangle \approx D_{298}(R_1 - R_2) + \langle E_v(R_1)\rangle + \langle E_v(R_2)\rangle$.

TABLE 3: Comparison of Calculated and Experimental Rate Constants[a]

			calculated results			
molecule	k_a(exptl‡)[b]	$\langle E\rangle$	preexp factor[b,c]	$s^{\ddagger d}$	k_a[b,e]	E_0[e]
$CH_3CH_2CH_2Cl$ (−HCl)	87 ± 3	90 ± 1	1.37 (1.34) (0.61)	2	104	54.0
$CD_3CD_2CH_2Cl$ (−DCl)	22 ± 1	90.5 ± 1	1.21 (1.29)(0.56)	2	27	55.1
$CF_3CH_2CH_2Cl$ (−HCl)	12 ± 2	101 ± 2	0.82 (1.02)[f] (0.48)	2	13	58
	2.4 ± 0.2	94 ± 2			2.8	58
(−HF)	0.030 ± 0.011	94 ± 2	0.70 (1.06) (0.32)	6	0.017−0.050[g]	72−70[g]
$CF_3CH_2CH_3$ (−HF)	25 ± 3	101 ± 2	1.0 (1.17) (0.41)	6	17	64
	4.0 ± 0.4	94 ± 2			3.9	
$CF_3CH_2CF_3$ (−HF)	0.13	104 ± 2	1.0 (1.14) (0.40)	12	0.15	73
$CH_3CH_2CH_2F$ (−HF)	17 ± 2	94 ± 2	0.70 (1.24) (0.27)	2	20	59
CH_3CHFCD_3 (−HF)	71 ± 10	95 ± 2	0.68 (1.13) (0.29)	3	70	55.0
(−DF)	47 ± 7	95 ± 2	0.58 (1.11) (0.25)	3	47	55.9
$CH_3CF_2CH_3$ (−HF)	5200	116−120[h]	0.67 (1.14) (0.28)	12	4400−6400[h]	55
	7080	117−121[h]			5000−7000[h]	

[a] Energies are in kcal mol^{-1}; rate constants and preexponential factors are s^{-1}. [b] Entries for k_a should be multiplied by 10^6, and those for the preexponential factor, by 10^{13}. [c] In partition function form per unit reaction path with the torsional motions treated as hindered internal rotations. The numbers in parentheses are $Q_R^\ddagger/Q_R$ and $Q_v^\ddagger/Q_v$; the latter includes partition functions for HIR. The calculations are at 1000 K for HF elimination and 800 K for HCl elimination. [d] Reaction path degeneracy. [e] Given the uncertainties in k_a(exptl) and $\langle E\rangle$, forcing an exact match between k_a(exptl) and k_a(calcd) has no significance. Therefore, E_0 values (two significant figures) were selected that provided k_a(calcd), which were within ~20% of the experimental result. Three significant figures are necessary for the representation of isotope effects for $C_2H_5CH_2Cl$, $C_2D_5CH_2Cl$, and CH_3CHFCD_3. [f] This ratio, which is unusually small for an HCl-elimination rate constant, is a fortuitous result for the gauche conformer. The moment of inertia ratio for the trans conformer is 1.21. [g] The range for E_0 corresponds to the listed calculated rate constant that matches the ±30% uncertainty in k_a(exptl). [h] The limits to $\langle E\rangle$ arise from a lack of knowledge about the vibrational excitation of CH_2 (see the text) and not from the uncertainty of the thermochemistry of CH_3CHF_2 or $CH_3CF_2CH_3$.

standard method is not as reliable as direct D/S versus pressure measurements, the plots[9] of the data appear to be satisfactory for this type of experiment. We have selected data from the mid-temperature range (60 and 100 °C), which give rate constants of 330 and 450 Torr.

C. Evaluation of the Thermochemistry. To find average energies of the chemically activated molecules, the enthalpy of formation of the recombining radicals, CF_3, C_2H_4Cl, CH_2Cl, CF_3CH_2, C_2H_5, and C_2D_5, plus the ΔH_f° ($CF_3CH_2CH_2Cl$) and ΔH_f° (*n*-C_3H_7Cl) are needed for eq 8.[25−33]

$$\langle E\rangle = \Delta H^\circ_{f0}(R_1{-}R_2) - \Delta H^\circ_{f0}(R_1) - \Delta H^\circ_{f0}(R_2) + \langle E_{300}\rangle = D_0(R_1{-}R_2) + \langle E_{300}\rangle \quad (8)$$

In eq 8, we have assumed that the activation energy for the $R_1 + R_2$ recombination is zero. The $\langle E_{300}\rangle$ term is the average thermal energy of the formed molecules, which ideally would be obtained from their thermal distribution. We have estimated $\langle E_{300}\rangle$ from the average thermal energy of R_1 and R_2 as $3RT + \langle E_v(R_1)\rangle + \langle E_v(R_2)\rangle$ where E_v is the vibrational energy. This estimate for $\langle E_{300}\rangle$ has less uncertainty than the uncertainty of the ΔH_f° values. In fact, $\langle E\rangle$ can be closely estimated as $D_{298}(R_1{-}R_2) + \langle E_\nu(R_1)\rangle + \langle E_\nu(R_2)\rangle$. The ΔH°_{f298} values with sources are tabulated in Table 3. With the exception of ΔH_f°($CF_3CH_2CH_2Cl$), the enthalpies of formation are based upon experimental evidence, and the values seem to be reliable. We estimated ΔH_f°($CF_3CH_2CH_2Cl$) by assuming that D(CF_3-CH_2CH_2−H) and D($CF_3CH_2CH_2$−Cl) were the same as for propane and *n*-propyl chloride.

The $\langle E\rangle$ values for reactions previously reported in the literature were reexamined, and the selected values are in Table 3. The average energies previously assigned[1] to $CF_3CH_2CF_3$ and to $CF_3CH_2CH_3$ are bascially satisfactory, although the 95 kcal mol^{-1} value for $CF_3CH_2CH_3$ was lowered to 94 kcal mol^{-1}. The $\langle E\rangle$ for *n*-propyl fluoride was assigned as 94 ± 2 kcal mol^{-1} from the enthalpies of formation of CH_2F,[28] C_2H_5,[30] and CH_3-CH_2CH_2F.[31c,32] The $\langle E\rangle$ for CH_3CHFCH_3 was assigned from the enthalpies of formation of CH_3,[30] CH_3CHF,[28] and CH_3-$CHFCH_3$.[32,33] Although the $\Delta H_f^\circ(CH_2(\tilde{a}^1A_1))$ is now known, assigning $\langle E\rangle$ from reaction 9 is still somewhat uncertain.

$$CH_2(\tilde{a}^1A_1) + CH_3CHF_2 \rightarrow CH_3CF_2CH_3 \qquad \Delta H^0_{298} = -113 \text{ kcal mol}^{-1} \quad (9)$$

The enthalpy of reaction was obtained from $\Delta H_f^\circ(CH_2,\tilde{a})^{27b} = 102.4$, $\Delta H_f^\circ(CH_3CHF_2)^{27a} = -118.8$, and $\Delta H_f^\circ(CH_3CF_2CH_3)^{25} = -129.8$ kcal mol^{-1}. Adding the thermal energy gives $\langle E\rangle = 116$ and 117 kcal mol^{-1} at 60 and 100 °C. Depending upon experimental conditions, the CH_2 radicals from the photolysis of ketene may retain excess energy as vibrational excitation. If, on average, one bending mode was excited, then the $\langle E\rangle$ would be increased by 3.8 kcal mol^{-1}. Thus, we have used 116−120 and 117−121 kcal mol^{-1} as the energy for $CH_3CF_2CH_3$.

Calculated Results

A. Computational Methods. The objective is to calculate values for $k_{\langle E\rangle}$ using frequencies and moments of inertia from electronic structure calculations, the $\langle E\rangle$ from thermochemistry, and selected (assumed) threshold energies, E_0. With this approach, the only variable in fitting the calculated $k_{\langle E\rangle}$ to the experimental rate constant is E_0. The method is demonstrated in the Appendix for CH_3CF_3, CH_3CH_2F, and CH_3CH_2Cl.

Electronic structure calculations were made with the Gaussian 03 suite of programs.[34] Vibrational frequencies and principal

moments of inertia were calculated for the molecules and transition states using density-functional theory, method B3PW91, with two basis sets, 6-31G(d′,p′) and 6-311+G(2d,p), for the CF_3CH_3, C_2H_5F, C_2H_5Cl, *n*-C_3H_7Cl, and $CF_3CH_2CH_2Cl$ molecules and transition states. The calculated frequencies and geometries of the transition states and molecules for $C_2H_5CH_2Cl$, $C_2D_5CH_2Cl$, and $CF_3CH_2CH_2Cl$ are provided in Supporting Information. Comparisons were made between calculated frequencies from both basis sets with experimentally measured frequencies, including conformers of *n*-C_3H_7Cl and *n*-C_3H_7F; the agreement was excellent, even for low frequencies, with both basis sets. The frequencies of the transition states were nearly identical from both basis sets; their vibrational partition functions and sums of states differed by ≤15%. The transition states for HF and HCl elimination from fluoro- and chloroethane have been analyzed at several levels of theory.[13,14] In fact, the transition-state structure is not very sensitive to the level of theory, and the bond distances in the planar HCCX ring can be described as a 35−40% extension of R_{C-X}, a 7−8% contraction of R_{C-C}, and a 15−17% extension of R_{C-H}; R_{H-X} is 40−45% larger than the equilibrium R_{H-X} value. The out-of-ring geometry is close to that of the product olefin. These generalizations also are confirmed by material in the Supporting Information for C_3H_7Cl and $CF_3CH_2CH_2Cl$. For $CF_3CH_2CF_3$ and $CF_3CH_2CH_3$, the calculated results from 6-31G(d′,p′) were compared with the 6-311G(2d,p) basis set; the calculated frequencies were very similar. The important conclusion from this paragraph and the material in the Supporting Information is that the frequencies of the transition state are not sensitive to the basis set of the calculation. In an effort to be systematic, all rate constants were calculated with frequencies and moments of inertia from the 6-31G(d′,p′) basis set.

Thermal preexponential factors and RRKM rate constants were calculated from standard[11] transition-state theory equations.

$$k(T) = \frac{s^{\ddagger} kT}{h}\left(\frac{Q_R^{\ddagger}}{Q_R}\right)\left(\frac{Q_v^{\ddagger}}{Q_v}\right)\exp\left(-\frac{E_0}{RT}\right) \qquad (10)$$

$$k_E = \frac{s^{\ddagger}}{h}\left(\frac{I^{\ddagger}}{I}\right)^{1/2}\frac{\sum P^{\ddagger}(E-E_0)}{N_E^*} \qquad (11)$$

The torsional modes can be treated as vibrations, free internal rotors, or hindered internal rotors (HIR). These choices are examined for CF_3CH_3, CH_3CH_2F, and CH_3CH_2Cl in the appendix. Because the hindered internal rotor is the most realistic choice, the reported values for the preexponential factor and $k_{\langle E\rangle}$ for the fluorochloropropanes will be for hindered-rotor models. One advantage of treating torsional modes as hindered rotations is that the reaction path degeneracy, $s^{\ddagger}$ is naturally identified. In eq 10, the vibrational partition function ratio, $Q_v^{\ddagger}/Q_v$, includes the contribution from torsional modes. In eq 11, $(I^{\ddagger}/I)^{1/2}$, the square root of the ratio of the moments of inertia, is the same as $Q_R^{\ddagger}/Q_R$ because we treated the three overall rotations as adiabatic. For the convenience of the reader, the $(I^{\ddagger}/I)^{1/2}$ ratio and the $Q_v^{\ddagger}/Q_v$ ratio, with the torsional modes treated as hindered rotors, are reported with the preexponential factor in Table 3. The symmetry number of the HIR of the molecule that becomes a vibrational mode in the four-centered transition state was always set equal to 1 in the calculations. The symmetry number of the second HIR is the same for the molecule and transition state and, hence, cancels.

The principal axes of rotation were identified and combined with the axes of the rotating top (internal rotor) to find the reduced moment of inertia, I_{red}, for each internal rotation using the methods of Pitzer.[35] For some molecules, the I_{red} values were taken from the literature. The tables provided by Pitzer were used to find Q_{HIR} from I_{red}, V, and temperature.

Calculations of the sums of states for the transition state, $\sum P^{\ddagger}(E - E_0)$, and densities of states for the molecule, N_E^*, were made with the Multi-Well code, furnished by courtesy of Professor Barker. This code has an option that permits the treatment of torsional modes as hindered internal rotors in the calculation of sums and densities of states. The $I^{\ddagger}_{red}$ for the transition state is very similar to the corresponding I_{red} in the molecule, and the $I^{\ddagger}_{red}$ values will not be cited unless the difference is significant. The potential energy barriers, V, for internal rotation for the molecule were taken from the literature; these barriers for CH_3 or CF_3 groups in the transition states were assumed to be the same as for the molecule.

The application of eq 11 presupposes fast internal vibrational relaxation (IVR). For the time scale (10^{-7}s) of the reactions in this study, IVR surely will have occurred, and statistical treatment of the internal energy states should be valid. Nevertheless, IVR continues to be a subject for debate, and Keifer and co-workers[36] have raised this question for CH_3CF_3 in high-termperature experiments. However, extremely short IVR times (on the order of picoseconds) have been demonstrated by direct measurements for halogenated ethane molecules.[37]

Before presenting the calculated results for each molecule, some general properties of the three options (vibration, hindered rotor, and free rotor) for treating torsional motions will be noted. The difference is most important for the thermal activation preexponential factor because $Q_{vib} < Q_{HIR} < Q_{FR}$. Thus, the rule of thumb[11] regarding selection of a transition state for RRKM calculations that matches the thermal preexponential factor requires careful evaluation of the torsional modes. Stein and Rabinovitch[38] showed that values of the density of internal states for ethane ($I_{red} = 1.60$ amu-Å^2, $\sigma_{IR} = 3$) actually were similar for all three methods for energies above 60 kcal mol^{-1}. The internal rotational barrier is only 2.9 kcal mol^{-1} in C_2H_6, and the density of states for the hindered rotor equaled that of the free rotor at energies above ∼90 kcal mol^{-1}. Because the harmonic oscillator levels are equally spaced whereas those for a rotor change as $E_R^{1/2}$, the density of the vibrational ($\nu = 285$ cm^{-1}) model actually slightly exceeded that of the free-rotor model for energies above 85 kcal mol^{-1}. The situation for CH_3CH_2F (see Appendix) with a barrier of 3.34 kcal mol^{-1} and $I_{red} = 2.60$ amu-Å^2 is very similar; above 60 kcal mol^{-1}, the density of states for the vibrational ($\nu = 262$ cm^{-1}) model is nearly the same as that for the hindered rotor, and both approach the free-rotor limit above ∼80 kcal mol^{-1}. It follows that the larger rate constant for the vibrational model, which is a factor of 3 at 90 kcal mol^{-1} for CH_3CH_2F, arises from the assumed reaction path degeneracy for the vibrational model (i.e., if $s^{\ddagger} = 1$ was chosen for the vibrational model, then the k_E values for vibration, HIR, and free rotation would be nearly the same). The larger E_0 values needed to fit the chemical activation rate constants for the vibrational models of CF_3CH_3, CH_3CH_2F, and CH_3CH_2Cl (see Appendix) are just a consequence of the assumed reaction path degeneracy. The reaction path degeneracy arises naturally from the symmetry number ($\sigma_{IR} = 3$) for the hindered internal methyl rotor.

The I_{red} (∼50 amu-Å^2) is much larger, and the vibrational torsional frequency (∼60 cm^{-1}) is much lower for a CF_3 group. The large variation in the torsional frequency and I_{red} for CF_3 groups in different chemical environments requires a case-by-case comparison of the vibrational and HIR models. Nevertheless, above 60 kcal mol^{-1} the density of states for the CF_3 free

rotor usually was less than a factor of 2 larger than for the vibration model. For a barrier of 4.5 kcal mol^{-1}, the density of states for the hindered CF_3 rotor was typically ~40% larger than for the vibrational model in the 80−100 kcal mol^{-1} range. At energies of 90−100 kcal mol^{-1}, the density of states for the hindered CF_3 rotor was still 20−30% smaller than that of the free rotor.

The situation for the unsymmetric rotors, CH_2Cl and CH_2F, differs from the symmetric cases. The density of states for the hindered CH_2Cl rotor (I_{red} = 12 amu-Å^2, V = 4.0 kcal mol^{-1}) of *n*-C_3H_7Cl does approach the free-rotor limit at ~100 kcal mol^{-1}. However, the density of states for the hindered rotor is larger than that for the vibrational model (ν = 137 cm^{-1}) by a factor of 2.7 over the 80−100 kcal mol^{-1} range.

Because the barriers to internal rotation are relatively small compared to $\langle E\rangle$ or $\langle E\rangle - E_0$ and because the trends are similar for $\sum P^{\ddagger}(E - E_0)$ and N_E*, the rate constants from the HIR model usually were quite similar (20%) to those of the FR model. However, all results to be quoted in Table 3 are for torsions treated as hindered internal rotors.

B. Assignment of Threshold Energies. *B.1. $CF_3CH_2CH_3$, $CF_3CH_2CF_3$, and $CH_3CH_2CH_2F$.* These three fluoropropanes will be discussed together because they correspond to CH_3 or CF_3 substitution of CF_3CH_3 or CH_3 substitution of CH_3CH_2F. Methyl substitution of CF_3CH_3 giving $CF_3CH_2CH_3$ increased N_E*, relative to CF_3CH_3, by 4 orders of magnitude at 90 kcal mol^{-1}. The $\sum P^{\ddagger}(E - E_0)$ increased by 2 orders of magnitude for E_0 = 60 kcal mol^{-1}, and the rate constant would be expected to decrease by approximately 2 orders of magnitude with CH_3 substitution for a common E_0 and $\langle E\rangle$ for the pair of molecules. The same comparison for CF_3 substitution of CF_3CH_3 shows that N_E* increased by a factor of ~3 × 10^7 and $\sum P^{\ddagger}(E - E_0)$ increased by a factor of ~6 × 10^4 so that the rate constant of $CF_3CH_2CF_3$ would decrease by a factor of ~500 from just these statistical effects. Although these are large changes, eq 11 faithfully monitors these statistical effects because we have reliable vibrational frequencies for the molecules and transition states.

The calculated vibrational frequencies for $CF_3CH_2CH_3$ were similar to those recommended by Yamada et al.[31c] The internal rotational moments of inertia are 3.06 and 18.9 amu-Å^2 with barriers of 3.2 and 4.5 kcal mol^{-1} for the CH_3 and CF_3 rotors, respectively. The preexponential factor in Table 3 is only slightly larger than that for CF_3CH_3. Good overall agreement with the experimental rate constants of 25 and 4.0 × 10^6 s^{-1} at 101 and 94 kcal mol^{-1} is obtained for an E_0 of 64 kcal mol^{-1}, which is 4 kcal mol^{-1} below that for CF_3CH_3. The calculated ratio (4.7) does underestimate the experimental ratio (6.2) of rate constants for the two energies, which may suggest that the difference in $\langle E\rangle$ is more than 7.0 kcal mol^{-1}. A 2 kcal mol^{-1} change in E_0 changes k_E by a factor of 2.2, and a 2 kcal mol^{-1} change in $\langle E\rangle$ changes k_E by a factor of 1.6.

The calculations for $CF_3CH_2CF_3$ were made with two CF_3 rotors in the molecule and one in the transition state. Each had I_{red} = 51.6 amu-Å^2 and a 4.5 kcal mol^{-1} barrier. The experimental rate constant is 100 times smaller than for $CF_3CH_2CH_3$, and an E_0 of 73 kcal mol^{-1} is required to match the rate constant. Because $\langle E\rangle$ = 104 kcal mol^{-1} could be an overestimate, 73 kcal mol^{-1} may be an upper limit to E_0. Nevertheless, substitution of a CF_3 group in CF_3CH_3 *raises* the threshold energy by ~5 kcal mol^{-1}, whereas substitution of CH_3 *lowers* E_0 by ~4 kcal mol^{-1}.

The calculations for $CH_3CH_2CH_2F$ with the 6-31G(d′,p′) basis set were straightforward, and the calculated frequencies for the molecule agree with experimental results[39] and with Bozzelli's tabulation.[31c] The I_{red} values were 9.2 and 2.7 amu-Å^2, with barriers of 3.8 and 2.7 kcal mol^{-1} for the CF_3 and CH_3 groups, respectively.[31c,39,40] The CH_2F rotor was treated as a symmetric rotor because the barrier heights separating the trans and gauche conformers are similar.[31c,39] Rate constants were calculated with frequencies of the gauche conformer because the gauche conformer is 0.3 kcal mol^{-1} lower in energy than the trans conformer. Fitting the calculated rate constant to k_a(exptl) favored E_0 = 59 kcal mol^{-1}. The recombination of CH_2F and C_2H_5 was studied[10] over a broad range of temperature, and the calculated rate constants are in accord with the energy dependence of the experimental results. A thermal pyrolysis study[41,42] of $CH_3CH_2CH_2F$ reported Arrhenius constants of 1.8 × 10^{13} s^{-1} and E_a = 58.3 ± 1.0 kcal mol^{-1}, which would correspond to $E_0 \approx$ 56.5 ± 1.0 kcal mol^{-1} and a preexponential factor of ~0.3 × 10^{13} per path. Thus, the chemical and thermal activation data both suggest that CH_3 substitution in the β position of CH_3CH_2F lowers E_0 by ≤2 kcal mol^{-1}.

B.2. CH_3CHFCD_3 and $CH_3CF_2CH_3$. The calculated frequencies for CH_3CHFCD_3 and $CH_3CF_2CH_3$ matched the experimental recommendations.[43,44] The reduced moments of inertia for internal rotation are 3.04 and 5.74 amu-Å^2 for CH_3CHFCD_3 and 3.08 amu-Å^2 for $CH_3CF_2CH_3$. The barriers[43,44] for internal rotation for both molecules were taken as 3.2 kcal mol^{-1}. The preexponential factors per reaction path for $CH_3CF_2CH_3$ and CH_3CHFCD_3 are similar to those for other fluoroalkanes.

Threshold energies for molecules with halogen atoms in secondary positions are lower than their primary counterparts. The Arrhenius constants[42] for CH_3CHFCH_3 are 10$^{13.36}$ s^{-1} and 53.9 ± 1.0 kcal mol^{-1}, and a threshold energy of ~53 kcal mol^{-1} is expected for HF elimination with that for DF elimination being ~1.0 kcal mol^{-1} higher. Fitting the $k_a(-HF)$ experimental rate constant of CD_3CHFCH_3 required E_0 = 55 kcal mol^{-1}. The difference in zero-point energies (0.92 kcal mol^{-1}) gives a threshold energy of 55.9 kcal mol^{-1} for DF elimination with $k_a(-HF)/k_a(-DF)$ = 1.49, which is in excellent agreement with the experimental ratio (1.51). The *intramolecular* kinetic isotope effect is just the ratio of $\sum P_H^{\ddagger}(E - E_{0,H})/\sum P_D^{\ddagger}(E - E_{0,D})$, and properties of the molecule are not relevant. In fact, the calculated ratio did not depend on whether the CH_3 and CD_3 torsional motions were treated as vibrations or as internal rotors. The difference in $E_{0,H}$ and $E_{0,D}$ is the most important aspect of the isotope effect. The *intermolecular* kinetic isotope ratios for CH_3CHFCH_3 versus CD_3CHFCH_3 are dominated by the $N(E_D^*)/N(E_H^*)$ ratio, which is 7.0. After adjustment to a common reaction path degeneracy of 3 and with E_0 = 55 kcal mol^{-1} for CH_3CHFCH_3, the calculated ratios are $k(C_3H_7F, -HF)/k(CD_3CHFCH_3, -HF)$ = 1.5 and $k(C_3H_7F, -HF)/k(CD_3CHFCH_3, -DF)$ = 2.4.

As far as we know, the threshold energy for $CH_3CF_2CH_3$ has not been directly measured by thermal activation. Generally, multiple F atom substitution on the same carbon atom raises E_0 values. Fitting the $CH_3CF_2CH_3$ rate constants listed in Table 3 required an E_0 of 55 ± 1 kcal mol^{-1} for the hindered-rotor model. If a vibrational model had been used for the torsional modes, an E_0 of 58 kcal mol^{-1} would have been required. McDoniel and Holmes[2] previously employed these data[9] with a smaller collision diameter to assign an E_0 of 54 kcal mol^{-1} based on RRKM calculations using a vibrational model with a tighter transition state. The reliability of the E_0 = 55 kcal mol^{-1} value is difficult to judge because of limitations of the experiment. In the absence of other data, we tentatively conclude

that the threshold energies for HF elimination seem to be comparable for $CH_3CF_2CH_3$ and CH_3CHFCD_3.

B.3. $CH_3CH_2CH_2Cl$, $CD_3CD_2CH_2Cl$, and $CF_3CH_2CH_2Cl$. Thermal activation studies[45] provide Arrhenius constants of 3.2 ($\pm$1.6) $\times$ 10^{13} s^{-1} and E_a = 55.1 $\pm$ 0.7 kcal mol^{-1} for $CH_3CH_2CH_2Cl$, and methyl substitution in the β position of C_2H_5Cl lowered the activation energy by only 1$-$2 kcal mol^{-1}. Upon the basis of this thermal study, a threshold energy of 54 $\pm$ 1 would be expected for n-C_3H_7Cl with a preexponential factor of $\sim$0.6 $\times$ 10^{13} s^{-1} per path.

The calculations gave structures and frequencies, which are presented in the Supporting Information, for $CH_3CH_2CH_2Cl$ that closely matched the comprehensive experimental summary provided by Durig, Zhu, and Shen[46] for the trans and gauche conformers. Because the properties of both conformers are very similar and because the difference in energy between the conformers is only 52 $\pm$ 11 cm^{-1}, rate constants were calculated for the gauche conformer. These authors[40,46] also provide detailed information for I_{red} and the barriers for internal rotation of the CH_2Cl group. Fortunately, the barriers between the conformers are not very different, and we treated the CH_2Cl rotor as a symmetric rotor with a barrier of 4.0 kcal mol^{-1} and I_{red} = 12.2 amu-Å^2. The I_{red} and V[45c] were 2.7 amu-Å^2 and 2.9 kcal mol^{-1}, respectively, for the CH_3 rotor; however, the effects of the methyl rotor tend to cancel in the molecule and the transition state. The experimental rate constant of 8.7 $\times$ 10^7 s^{-1} at 90 kcal mol^{-1} was fitted with a threshold energy of 54 kcal mol^{-1}, although an E_0 of 55 kcal mol^{-1} would be equally acceptable.

The kinetic isotope effect for $C_2D_5CH_2Cl$ is a combination of a primary effect and a statistical secondary effect of the other four D atoms. The primary effect is largely the 1.1 kcal mol^{-1} difference in $E_{0,D} - E_{0,H}$. The statistical effect is defined in eq 12; the density ratio of $\sim$30 is reduced by the ratio of the sums of states.

$$\frac{k_H}{k_D} = \frac{(I_H)}{(I_D)} \times \frac{\Sigma P_H^{\ddagger}(E - E_{0,H})}{\Sigma P_D^{\ddagger}(E - E_{0,D})} \times \frac{N(E_D^*)}{N(E_H^*)} \qquad (12)$$

The calculation, which includes the 0.5 kcal mol^{-1} difference in average energies, has no adjustable parameters and gives k_H/k_D = 3.85, in agreement with the experimental result of 3.95 $\pm$ 0.2. The calculated kinetic isotope effect for the vibrational model was 3.9. The kinetic isotope effect is more sensitive to slight differences in average energies and threshold energies than the model for the torsional modes.

The $k(-HCl)$ for $CF_3CH_2CH_2Cl$ also can be discussed with the aid of eq 12 (with fluorine playing the role of D). The CF_3 group greatly increases the density of states, and $N_E^*(CF_3CH_2CH_2Cl)/N_E^*(CH_3CH_2CH_2Cl)$ = 4.2 $\times$ 10^3 at 95 kcal mol^{-1}. By analogy to $CF_3CH_2CF_3$ versus CH_3CF_3, substitution of a CF_3 group in ethyl chloride may raise the E_0 above the threshold energy of CH_3CH_2Cl (55 kcal mol^{-1}) for HCl elimination. The calculated frequencies of $CF_3CH_2CH_2Cl$, which can be found in the Supporting Information, were in accord with reported results.[47] Because the trans conformer is more stable by about 1 kcal mol^{-1}, the rate constant calculations were made with frequencies of the trans conformer. The I_{red} values for the rotors depend on the conformer geometry, and we adopted average values of I_{red} = 32 and 24.3 amu-Å^2 with V[31,47] = 4.5 and 5.0 kcal mol^{-1} for the CF_3 and CH_2Cl rotors, respectively. The I_{red} for CF_3 in the HCl transition state increased to 48.0 amu-Å^2; the I_{red} for CH_2Cl in the HF transition state remained at 24.3 amu-Å^2. The experimental rate constants at both energies could be matched with E_0 = 58 kcal mol^{-1}. The calculated ratio of rate constants for HCl elimination at 94 and 101 kcal mol^{-1} is 4.6. Because the experimental rate constant measured at 101 kcal mol^{-1} was an upper limit due to the chemical complexity of the photochemical system, the degree of agreement with the experimental ratio (5.0) is satisfactory. Exchange of a CF_3 group for a CH_3 did raise the threshold energy relative to that for $CH_3CH_2CH_2Cl$ (54 kcal mol^{-1}). The factor of 36 reduction in $k(-HCl)$ for $CF_3CH_2CH_2Cl$ versus $CH_3CH_2CH_2Cl$ arises mainly from the increased density of states from the substitution of three hydrogen atoms by three fluorine atoms; the 4 kcal mol^{-1} higher E_0 adds another factor of 0.28.

The HF elimination rate constant is 80 times smaller than the HCl elimination rate constant at 94 kcal mol^{-1}. Because the CF_2=$CHCH_2Cl$ product yield was small, the ratio has a 30% uncertainty. The HF elimination transition state was difficult to define in the DFT calculations largely because the asymmetric CH_2Cl rotor adds conformers to the transition state. We did the calculation with the frequencies of the most stable conformer of the transition state. As shown in Table 3, the HF- and HCl-elimination transition states for $CF_3CH_2CH_2Cl$ actually have very similar preexponential factors and ratios of partition functions. The experimental rate constants, which cover the range of (3.4 $\pm$ 1.1) $\times$ 10^4 s^{-1}, were fitted with a threshold energy of 70$-$72 kcal mol^{-1}, which is between the E_0 values for CF_3CH_3 and $CF_3CH_2CF_3$. According to our estimate for the rate constant for Cl atom rupture from $CF_3CH_2CH_2Cl$ at an energy of 101 kcal mol^{-1}, C$-$Cl bond rupture should not be competitive with HF elimination.

C. Comparison of Threshold Energies with Results from DFT Calculations. In the current work, the threshold energies were assigned by matching the experimental chemical-activation rate constants with the RRKM calculated value. The intrinsic uncertainty in an E_0 assignment from a single k_a(exptl) is estimated to be $\pm$2.0 kcal mol^{-1}. A 2 kcal mol^{-1} change in E_0 changes the rate constant for fluoropropanes by a factor of $\sim$2.5. The uncertainty of $\pm$2 kcal mol^{-1} is assigned by the following logic. The experimental plot of D/S versus inverse pressure, which gives k_a(exptl), generally has a $\pm$20% absolute uncertainty. The value of the experimental rate constant also depends on the collisional deactivation efficiency and the collision cross section. The deactivation efficiency for alkyl iodide molecules has not been measured for fluoropropanes or fluoroethanes. However, the deactivation of fluoroethanes and chloroethanes has been studied for CH_3Cl, CF_4, C_2F_6, and SF_6 as bath gases. Irrespective of the specific deactivation model, the limiting high-pressure rate constants for these molecules are only 25% larger than the unit deactivation limit, and we expect the alkyl iodides to have equal or greater collisional efficiency.[15$-$17] The more important variable actually is the collision cross section.[19,20] Thus, the total uncertainty in k_a(exptl) is assigned as $\pm$50%. If isotopic data or reliable measurements of k_a(exptl) at more than one energy or with more than one bath gas are available, then this uncertainty can be reduced somewhat. The calculated values for k_E also have uncertainty. First, $\langle E \rangle$ can have an uncertainty of $\pm$2 kcal mol^{-1}, and changing E from 95 to 97 kcal mol^{-1} changes k_E by $\sim$1.6 for fluoropropanes. Second, the calculation itself is subject to the question of using harmonic sums and densities plus the usual assumptions of transition-state theory.[11] The absolute uncertainty associated with the E_0 values of $\pm$2 kcal mol^{-1} should be less when comparing threshold energies within a series of similar molecules.

Threshold energies also were calculated for each reaction by DFT with the 6-31G(d′,p′) and the 6-311+G(2d,p) basis sets,

TABLE 4: Comparison of Calculated and Experimental Threshold Energies[a,b] for HX Elimination

	HCl elimination[c]				HF elimination[c]	
molecule	6-311+G(2d,p)	6-31G(d′,p′)	experimental[d]		6-311+G(2d,p)	6-31G(d′,p′)
CH_3CH_2Cl	52.93	54.48	55			
$CH_3CH_2CH_2Cl$	trans-51.04	52.49				
	gauche-50.87	52.32	54			
$CF_3CH_2CH_2Cl$	trans-55.68	56.69	58	71	63.01(65.73)[e]	66.53(69.24)[e]
	gauche-54.15	55.38			61.48(64.20)[e]	65.22(67.93)[e]
CH_3CH_2F				58	54.97	59.20
CH_3CF_3				69	64.80	68.79
$CH_3CH_2CH_2F$					trans-53.97	58.61
				59	gauche-54.11	58.85
$CF_3CH_2CH_3$				64	64.54	68.83
CH_3CHFCH_3				55	51.86	56.57
$CH_3CF_2CH_3$				55	56.00	60.57
$CF_3CH_2CF_3$				73	63.82	66.60

[a] Obtained by subtracting the calculated electronic energies, including the zero-point energy, of the transition state and molecule obtained from DFT(B3PW91) with the basis sets stated above. [b] In units of kcal mol^{-1}. [c] The two entries are for the two basis sets used for the DFT calculations. [d] The left-hand side is for HCl elimination, and the right-hand side is for HF elimination. The uncertainty in E_0(exptl) is ±2 kcal mol^{-1}; see the text. [e] The HF-elimination transition state has three conformers corresponding to the rotation of the CH_2Cl- group. We were able to define only two of the three conformers. The lowest-energy conformer has the CH_2Cl group turned so that the C−Cl bond is aligned in the general direction of the F atom in the ring.

and the threshold energies assigned in this work are compared to those calculated from the two basis sets in Table 4. Previous efforts from this laboratory[3b,4,13] and others[14] have shown that the calculated threshold energies change with the level of theory, but not necessarily in a predictable pattern. Thus, an exact match with the experimental E_0 is not expected; rather the DFT calculated results can be examined for correspondence with trends in the experimentally based threshold energies. An inspection of Table 4 shows that the threshold energies from the 6-311+G(2d,p) basis set are always lower than those from the 6-31G(d′,p′) basis set. The latter are closer to the experimental result, even though the basis set is larger for 6-311+G(2d,p) than for 6-31G(d′,p′). Except for the $CF_3CH_2CH_2Cl$ (loss of HF), $CF_3CH_2CH_3$, $CF_3CH_2CF_3$, and $CH_3CF_2CH_3$ reactions, the calculated E_0 values from the 6-31G(d′,p′) basis set are in acceptable agreement with the experimentally derived values.

DFT does not seem to predict the increase in E_0 for HF elimination for CF_3 substitution of CF_3CH_3 to give $CF_3CH_2CF_3$ or for CH_2Cl substitution in CF_3CH_3 to give $CF_3CH_2CH_2Cl$. The DFT calculations predict little change in threshold energy upon methyl substitution for CH_3CH_2Cl and CH_3CH_2F, and the experimentally based E_0 values are in agreement. However, the same prediction for $CH_3CH_2CF_3$ relative to CH_3CF_3 is not in accord with experimentally based E_0 values. Stated another way, *calculated* threshold energies for the $CH_3CF_3-CH_3CH_2F$ and $CH_3CH_2CF_3-CH_3CH_2CH_2F$ pairs both differ by 10 kcal mol^{-1}, whereas the *experimental* result for the latter pair is only 5 kcal mol^{-1}. The experimental rate constant ratios for n-C_3H_7Cl versus C_2H_5Cl, n-C_3H_7F versus C_2H_5F, and $CF_3CH_2CH_3$ versus CF_3CH_3 also can be compared. The ratios for the first two pairs are ∼60, whereas the last pair has a ratio of only 13 (for energies of 101 ± 2 and 104 ± 2 kcal mol^{-1}). Additional experiments are probably needed for $CF_3CH_2CH_3$ before $E_0 = 64$ kcal mol^{-1} is accepted as being experimentally established. Both basis sets predict that the E_0 for $CH_3CF_2CH_3$ should increase by 4−5 kcal mol^{-1} relative to that for CH_3CHFCH_3, whereas the chemical activation data for $CH_3CF_2CH_3$ gives the same E_0 as for HF elimination from CH_3CHFCD_3. The chemical system[9] for the $CH_3CF_2CH_3$ experiments was complex, and new improved experiments are needed before reaching a conclusion about the best E_0 for $CH_3CF_2CH_3$.

Conclusions

The most important conclusion from this work is the general agreement between the threshold energies assigned from chemical activation rate constants and those deduced from Arrhenius activation energies for five reactions (C_2H_5Cl, C_2H_5F, CF_3CH_3, n-C_3H_7Cl, and n-C_3H_7F). These threshold energies were obtained by matching experimental and calculated rate constants; the latter are based upon transition-state structures calculated from DFT, with treatment of the torsional modes as hindered internal rotors. Upon the foundations of this demonstration, threshold energies were assigned to HCl- and HF-elimination rate constants measured in the 90−104 kcal mol^{-1} range for $CF_3CH_2CH_3$, $CF_3CH_2CH_2Cl$, $CF_3CH_2CF_3$, CH_3CHFCD_3, and $CH_3CF_2CH_3$. The assignment of threshold energies by comparison of RRKM rate constants to chemical activation rate constants measured at a single fixed energy in a bath gas that provides efficient vibrational deactivation seems to be as reliable (±2 kcal mol^{-1}) as conventional measurements by thermal activation. To attain this goal, an accurate evaluation of the sums of states of the transition state and density of states of the molecule is required for the RRKM rate constant, and we recommend that torsional motions be treated as hindered internal rotors. The intermolecular kinetic isotope effect (4.0) for $C_2D_5CH_2Cl$ versus $C_2H_5CH_2Cl$ is mainly a statistical effect arising from the increased density of states for $C_2D_5CH_2Cl$. The large reduction in the HCl elimination rate constant (∼30) for $CF_3CH_2CH_2Cl$ versus $C_2H_5CH_2Cl$ is mainly a consequence of the large increase in the density of states for a CF_3 group versus that for a CH_3 group. The intra- and intermolecular kinetic isotope effects and the variation of the rate constants with energy seem to be adequately represented by the RRKM calculations, as would be expected.[11]

Although the transition-state structures calculated from DFT have lower vibrational frequencies than the empirically selected transition states of earlier work,[5−8] treatment of the torsional motions in the molecule (and transition state) as hindered internal rotors provides adequate agreement with the thermal preexponential factors because the hindered internal rotors have larger partition functions than the corresponding vibrations. This compensation is not as satisfactory for HCl elimination rate constants as for HF elimination rate constants because the extended C−Cl distance generates more low bending frequencies in the HCl transition state than in the analogous HF

TABLE 5: Summary for CH_3CF_3, CH_3CH_2F, and CH_3CH_2Cl

	CH_3CF_3		CH_3CH_2F		CH_3CH_2Cl	
quantity	calcd	exptl	calcd	exptl	calcd	exptl
		A. Thermal Activation				
preexponential factor[a](10^{13} s^{-1})		1.5		0.45		0.42
(i) HIR model	0.73		0.73		0.98	
(ii) vibrational model	2.6		2.4		3.8	
ratio of $Q^{\ddagger}/Q^b$						
(i) HIR model	(1.14)(0.31)		(1.21)(0.29)		(1.43)(0.41)	
(ii) vibrational model	(1.14)(1.08)		(1.21)(0.94)		(1.43)(1.61)	
threshold energy, E_o[c](kcal mol^{-1})		69.1 ± 3.0		57.6 ± 1.5		54.9 ± 1.5
		B. Chemical Activation				
$\langle E \rangle$, kcal mol^{-1}		103.7 ± 1.0		94.0 ± 1.5		90.6 ± 1.0
k_a (10^8 s^{-1})		3.2 ± 0.3		25 ± 4		48 ± 8
(i) HIR model[d]	3.2 ($E_0 = 70$)		22($E_0 = 58$)		60($E_0 = 55$)	
(ii) vibrational model[d]	3.3 ($E_0 = 73$)		27($E_0 = 61$)		53($E_0 = 59$)	

[a] The preexponential factor in partition function form per unit reaction path at 1000 K for CH_3CF_3 and C_2H_5F and 800 K for C_2H_5Cl; the reaction path degeneracy is 9 for CH_3CF_3 and 3 for CH_3CH_2F and CH_3CH_2Cl. [b] Expressed as $(Q_R^{\ddagger}/Q_R)(Q_v^{\ddagger}/Q_v)$ [c] From thermal activation at 1000 or 800 K; $E_a = E_0 + RT + \langle E_v^{\ddagger} \rangle - \langle E_v \rangle$, and for the transition-state models of these reactions, the threshold energy is given by $E_a - 1.9$ kcal mol^{-1} (1000 K) and $E_a - 1.6$ kcal mol^{-1} (800 K). [d] The number in parentheses is the threshold energy required for the cited k_a and listed $\langle E \rangle$. At 95 kcal mol^{-1} of energy, a 2.0 kcal mol^{-1} change in E changes k_E by a factor of ~1.5, and a 2.0 kcal mol^{-1} change in E_0 changes k_E by a factor of 2.1.

transition state. Additional experimental tests[48] are needed to define the C−X extension in transition-state structures. The calculated RRKM rate constants at 90−100 kcal mol^{-1} are nearly the same whether the torsional motions are treated as free or hindered rotors.

Although the structures of the transition states calculated from the 6-311+G(2d,p) and 6-31G(d′,p′) basis sets were very similar, the calculated threshold energies from the 6-311+G(2d,p) basis set were 2−4 kcal mol^{-1} below the values from the 6-31G(d′,p′) basis set. The threshold energies from the 6-31G(d′,p′) basis set were close to the experimentally assigned values, except for HF elimination from $CF_3CH_2CH_2Cl$ and $CF_3CH_2CF_3$, which was about 4 kcal mol^{-1} too low, and for $CF_3CH_2CH_3$, which was 4 kcal mol^{-1} too high. Except for the simplest case, CF_3CH_3, these DFT calculations do not predict reliable threshold energies for HF-elimination reactions from molecules with CF_3 groups.

Acknowledgment. We thank Katie Burgess and Jay Simmons, Jr. for faithful assistance with the computations. We also thank Professor Barker, University of Michigan, for proving the Multi-Well computer code. Financial support for this work was provided by the U.S. National Science Foundation under grants CHE-9508666 and CHE-0239953.

Appendix

A. CF_3CH_3. Holmes and co-workers[13] have summarized the thermal activation data, and they recommended 3.5×10^{14} s^{-1} and 71 kcal mol^{-1} for the Arrhenius A factor and activation energy E_a. The uncertainty in E_a is ~3 kcal mol^{-1}, which corresponds to a factor of 4 in the A factor. We prefer to compare our transition-state calculations to preexponential factors in partition-function form and threshold energies. For our models of the transition state and molecule, $E_a - E_0$ is 1.9 kcal mol^{-1} at 1000 K. Thus, the preexponential factor becomes 1.4×10^{14} s^{-1}, and the threshold energy is 69.1 kcal mol^{-1}. We have adopted a reaction path degeneracy of 9, so the preexponential factor per unit path is 1.5×10^{13} s^{-1} at 1000 K with an uncertainty of a factor of 3−4.

The high-pressure chemical activation rate constant, k_a, measured from the recombination of CH_3 and CF_3 radicals has been studied in several laboratories and with a large number of bath gases. The best value for k_a is $3.2(\pm 0.3) \times 10^8$ s^{-1} with efficient bath gases.[16] An inspection of several recent reports dealing with the thermochemistry of fluoroethanes provides $D_{298}(CH_3-CF_3) = 102 \pm 1.0$ kcal mol^{-1}, which becomes 100.2 kcal mol^{-1} at 0 °K. Adding the thermal energy of the recombination gives $\langle E \rangle = 103.7 \pm 1.0$ kcal mol^{-1}.

Holmes and co-workers[13] investigated a range of ab initio and DFT calculations for the CF_3CH_3 reaction. They found that all calculations gave very similar vibrational frequencies and moments of inertia for the molecule, which matched experimental measurements, and for the transition state. This conclusion is confirmed by the models employed recently by Keifer[36] for the G-3 level of computation. We have used two basis sets in a DFT calculation, B3PW91/6-31G(d′,p′) and B3PW91/6-311+G(2d,p), and recalculated the frequencies and moments of inertia. Both basis sets gave essentially the same preexponential factor and RRKM-calculated k_E values. We have treated the torsional motion as a vibration ($\nu_{torsion} = 260$ cm^{-1}) and as a hindered rotor (V[49] = 3.12 kcal mol^{-1} and $I_{red} = 3.08$ amu-Å^2). For both models, the reaction path degeneracy was 9, and the internal rotational symmetry number ($\sigma = 3$) was deleted from calculations involving the hindered internal rotor. The method of Pitzer[35] was used to calculate the partition function for hindered rotation.

The calculations from the 6-31G (d′,p′) basis set are compared with the experimental data in Table 5. The ratio of vibrational partition functions for the transition state and molecule is 1.08 (vibrational model) or 0.31 (HIR model). Within the rather large uncertainty of the preexponential factors and E_0 values from thermal activation data, the calculated preexponential factor and assigned E_0 from the vibrational and hindered rotor models are both satisfactory. However, on balance we favor the hindered-rotor model, which requires a lower E_0 to match the chemical activation k_a and gives the smaller preexponential factor. The preexponential factor and k_a values (vibrational model) for the 6-311+G(2d,p) basis set were ~13% larger than those from the 6-31G(d′,p′) basis set.

B. C_2H_5F. Rajakumar and Arunan[14] have summarized the thermal activation studies. The three experiments, which cover the temperature ranges of 1280−1660, 1280−1660, and 684−739 K, give Arrhenius constants of 2.63×10^{13}, 4.67×10^{13}, and 2.0×10^{13} s^{-1} and 59.5, 58.2, and 59.5 kcal mol^{-1}. We adopt values of $A = 3.5 \times 10^{13}$ s^{-1} and $E_a = 59.5$ kcal mol^{-1}. At 1000 K, these values become 1.35×10^{13} s^{-1} for the

preexponential factor (partition-function form) and 57.6 kcal mol^{-1} for the threshold energy. In anticipation of a preference for the hindered-rotor treatment, we adopt a reaction path degeneracy of 3, and the preexponential factor per path becomes 0.45×10^{13} s^{-1}. The absolute uncertainty in E_0 is, at least, 1.5 kcal mol^{-1}, which corresponds to a factor of 2 in the preexponential factor. Several chemical activation studies have been made using the $CH_3 + CH_2F$ reaction. The most systematic study is by Richmond and Setser[15] with several bath gases. The unit deactivation rate constant is $25 \pm 4 \times 10^8$ s^{-1}. The ΔH°_{f298} (CH_3CH_2F) is a current subject of discussion. If $\Delta H^\circ_{f298}(CH_3CH_2F) = -65.5$ kcal mol^{-1}, favored by Smith[32] and by Luo and Benson,[33] is adopted, then $D_{298}(CH_3-CH_2F) = 90.7$ kcal mol^{-1} and $\langle E(CH_3CH_2F)\rangle = 94 \pm 1.5$ kcal mol^{-1}.

Calculations were made for CH_3CH_2F and its transition state using B3PW91 with 6-31G(d′,p′) and 6-311+G(2d,p) basis sets. The molecular frequencies and the moments of inertia for the molecule and for the transition state were very similar from both basis sets; they also are similar to those obtained by Rajakumar and Arunan.[14] The calculated frequencies for the molecule match those from experimental measurements. The internal rotor has a reduced moment of inertia of 2.60 amu-Å^2 with V[50] $= 3.35$ kcal mol^{-1}. The preexponential factor and the k_a calculated from the frequencies given by the 6-31G(d′,p′) basis set are shown in Table 5.

The calculated preexponential factors for CF_3CH_3 and CH_3CH_2F are very similar, indicating that the structures of the transition states are nearly identical. The preexponential factor for CH_3CH_2F from the hindered-rotor model agrees better with the experimental result than does the calculation from the vibrational model. The hindered-rotor calculation for k_a matches the experimental k_a for an E_0 of 58 kcal mol^{-1}, which is preferable to the 3 kcal mol^{-1} higher threshold energy required for a fit by the vibrational model.

C. C_2H_5Cl. Rajakumar and Arunan[14] have provided a summary of the numerous thermal-activation investigations of C_2H_5Cl. Because the majority of the investigations were experiments in static bulbs below 1000 K, we will make the comparison with calculations at 800 K. The agreement between the different experiments is actually quite good, and the average of the reports that seem most reliable (to us) gives $E_a = 56.5$ kcal mol^{-1} and $A = 3.5 \times 10^{13}$ s^{-1}. The uncertainty in E_a is probably 1.5 kcal mol^{-1}, even though the deviation among the studies is less, because the temperature range for each study was relatively narrow. The kinetic isotope effects[5a,b] have also been investigated, and the most recent study[18] with CH_2DCD_2Cl confirms the Arrhenius constants just mentioned, as well as a 1.1 kcal mol^{-1} difference in E_a for HCl versus DCl elimination. If we ignore the possible (vide infra) difference in the heat capacity of C_2H_5Cl and its transition state, then these Arrhenius parameters correspond to $E_0 = 54.9$ kcal mol^{-1} and a preexponential factor of 1.3×10^{13} s^{-1}. Dividing by the reaction path degeneracy of 3 gives 0.42×10^{13} s^{-1}, which is similar to the preexponential factor for C_2H_5F.

The chemical activation rate constant for C_2H_5Cl formed from $CH_3 + CH_2Cl$ has been measured in three independent experiments,[5,8] and the best value seems to be 48 ($\pm$8) $\times 10^8$ s^{-1} for unit deactivation. This value has been revised upward from the original report to be consistent with the collision diameters used in this paper (Table 1). The nonequilibrium kinetic isotope effects for CD_3CH_2Cl and CD_3CD_2Cl also have been measured,[5a,b] and the experimental results seem to be self-consistent. The $D_{298}(CH_3-CH_2Cl)$ is 89.8 $\pm$ 1.0 kcal mol^{-1}, and $\langle E\rangle = 90.6 \pm 1.0$ kcal mol^{-1} is based on reliable thermochemistry.

Frequencies and moments of inertia were calculated with the 6-31G(d′,p′) and 6-311+G(2d,p) basis sets, and the results were compared to those reported by Arunan and co-workers and by McGrath and Rowland.[49] The agreement among the calculations is very good, and the calculated frequencies of C_2H_5Cl match experimental measurements. We used a reduced moment of inertia of 2.78 amu-Å^2 with $V = 3.5$ kcal mol^{-1} for the hindered rotor.[50]

Comparison of the CH_3CH_2F and CH_3CH_2Cl calculated preexponential factors shows that the value for CH_3CH_2Cl is larger, even at 800 K. This trend is documented by comparison of the partition function ratios; the $Q_R^\ddagger/Q_R$ is surprisingly large (1.43) for CH_3CH_2Cl. The preexponential factor for the hindered-rotor model is 2 times larger than the experimental value for CH_3CH_2Cl. The calculated k_a for the hindered-rotor treatment satisfactorily agrees with the experimental result for $E_0 = 55$ kcal mol^{-1}. The vibrational model requires a higher threshold energy, and the comparison with the experimental data clearly favors a hindered-rotation treatment of the torsional motion. One point worth noting about the transition state is the extended C−Cl distance, which is 35−45% larger than a normal C−Cl bond. This bond extension of the heavy Cl atom increases the moments of inertia and introduces some low frequencies in the transition state. In particular, a frequency in the 675 cm^{-1} range for the molecule corresponds to a 375 cm^{-1} frequency in the transition state.

McGrath and Rowland[51] used ab initio electronic structure theory to calculate thermal rate constants for C_2H_5Cl and C_2D_5Cl. They favored results from the quadratic configuration interaction (QCISD) level of theory using a CC-PVDZ basis set. These authors chose to compare their computed thermal rate constants (with their threshold energy) to the rate constants of Heydtman and co-workers[52] over the 715 to 765 K range. They claimed good agreement because the calculated larger threshold energy (59.1 kcal mol^{-1}) was compensated by the calculated larger preexponential factor, relative to conventional experimental results,[14] and the calculated and experimental rate constants seemed to agree over the narrow temperature range of 715−765 K. In fact, the transition state of McGrath and Rowland is virtually identical to ours; their $Q_v^\ddagger/Q_v$ ratio at 800 K is 1.54 versus our value of 1.61. As noted by Rajakumar and Arunan,[14] the threshold energy and preexponential factor of McGrath and Rowland are both somewhat larger than conventional choices for the best experimentally based values. In some unpublished studies, Holmes and co-workers[53] have also investigated the C_2H_5Cl reaction. The calculations employed both DFT methods and ab initio methods (Moller−Plesset, complete basis set and Gaussian 2). The range of the preexponential factors (at 800 K) was from 3.3×10^{13} to 5.4×10^{13} s^{-1} (vibrational model) with the majority being $\sim 3.6 \times 10^{13}$ s^{-1}. Thus, all levels of calculation give a transition state with a very similar structure. If the frequencies of this structure are adopted for conversion of the experimental Arrhenius constants to a threshold energy and preexponential factor, then the values become $\sim$54.5 kcal mol^{-1} and 0.33×10^{13} s^{-1}, respectively. Both numbers are slightly smaller than the values given in Table 5, which makes the discrepancy between the calculated and experimental preexponential factors somewhat larger. Given the large number of experimental measurements for the Arrhenius parameters, the discrepancy between the calculated and experimental preexponential factor may suggest that the C−Cl bond length has been overestimated in the CH_3CH_2Cl transition state by all levels of electronic structure calculations.

Summary

(1) Transition-state structures for HCl and HF elimination calculated by DFT give preexponential factors that agree with experimental preexponential factors for C_2H_5Cl, C_2H_5F, and CF_3CH_3 to within the experimental uncertainty. Furthermore, the structures of the transition states are not very sensitive to the level of electronic structure calculation.

(2) These transition-state structures, with the torsional mode of the molecule treated as a hindered rotation, used with RRKM theory provide unimolecular rate constants that match experimental rate constants, measured at a fixed energy, for choices of threshold energies that agree with experimental threshold energies for CF_3CH_3, CH_3CH_2F, and CH_3CH_2Cl.

(3) Upon the basis of (1) and (2), we have employed transition-state structures calculated from DFT in RRKM calculations to assign threshold energies from the experimental chemical-activation rate constants for several fluoro-, chloro-, and fluorochloropropanes.

Supporting Information Available: Calculated frequencies and geometries of the transition states and molecules for $C_2H_5CH_2Cl$, $C_2D_5CH_2Cl$, and $CF_3CH_2CH_2Cl$. This material is available free of charge via the Internet at http://pubs.acs.org.

References and Notes

(1) Ferguson, H. A.; Ferguson, J. D.; Holmes, B. E. *J. Phys. Chem. A* **1998**, *102*, 5393.

(2) McDoniel, J. B.; Holmes, B. E. *J. Phys. Chem. A* **1997**, *101*, 1334.

(3) (a) Burgin, M. O.; Heard, G. L.; Martell, J. M.; Holmes, B. E. *J. Phys. Chem. A* **2001**, *105*, 1615. (b) Heard, G. L.; Holmes, B. E. *J. Phys. Chem. A* **2001**, *105*, 1622.

(4) Roach, M. S.; Sibila, B. M.; Holmes, B. E. *J. Phys. Chem. A*, submitted for publication, 2005.

(5) (a) Dees, K.; Setser, D. W. *J. Chem. Phys.* **1968**, *49*, 1193. (b) Clark, W. G.; Setser, D. W.; Dees, K. *J. Am. Chem. Soc.* **1971**, *93*, 5328. (c) Kerr, J. A.; Timlin, D. M. *Trans. Faraday Soc.* **1971**, *67*, 1376.

(6) (a) Chang, H. W.; Craig, N. L.; Setser, D. W. *J. Phys. Chem.* **1972**, *76*, 954. (b) Neely, B. D.; Carmichael, H. J. *J. Phys. Chem.* **1973**, *77*, 307.

(7) Kim, K. C.; Setser, D. W. *J. Phys. Chem.* **1973**, *77*, 2021.

(8) Dees, K.; Setser, D. W.; Clark, W. G. *J. Phys. Chem.* **1971**, *75*, 2231.

(9) Kerr, J. A.; Phillips, D. C.; Trotman-Dickenson, A. F. *J. Chem. Soc. A* **1968**, 1806.

(10) Kerr, J. A.; O'Grady, B. V.; Trotman-Dickinson, A. F. *J. Chem. Soc. A* **1969**, 275.

(11) (a) Robinson, P. J.; Holbrook, K. A. *Unimolecular Reactions* 1st and 2nd eds.; Wiley-Interscience: New York, 1972, 1996. (b) Steinfeld, J. I.; Francisco, J. S.; Hase, W. L. *Chemical Kinetics and Dynamics*, 1st and 2nd eds.; Prentice Hall: Saddle River, NJ, 1989, 1999. (c) Baer, T.; Hase, W. L. *Unimolecular Reaction Dynamics: Theory and Experiments*; Oxford University Press: New York, 1996.

(12) Toto, J. L.; Pritchard, G. D.; Kirtman, B. *J. Phys. Chem.* **1994**, *98*, 8359.

(13) Martell, J. M.; Beaton, P. T.; Holmes, B. E. *J. Phys. Chem. A* **2002**, *106*, 8471.

(14) Rajakumar, B.; Arunan, E. *Phys. Chem. Chem. Phys.* **2002**, *5*, 3897.

(15) Richmond, G.; Setser, D. W. *J. Phys. Chem.* **1980**, *84*, 2699.

(16) Marcoux, P. J.; Setser, D. W. *J. Phys. Chem.* **1978**, *82*, 97.

(17) (a) Chang, H. W.; Setser, D. W. *J. Am. Chem. Soc.* **1969**, *91*, 7648. (b) Setser, D. W.; Siefert, E. E. *J. Chem. Phys.* **1972**, *57*, 3613, 3623.

(18) Choi, C. J.; Lee, B.-W.; Jung, K.-H.; Tschuikow-Roux, E. *J. Phys. Chem.* **1994**, *98*, 1139.

(19) Hippler, H.; Troe, J.; Wendelken, H. J. *J. Chem. Phys.* **1983**, *78*, 6709.

(20) Mourits, F. M.; Rummens, F. H. A. *Can. J. Chem.* **1977**, *55*, 3007.

(21) Simons, J. W.; Rabinovitch, B. S. *J. Phys. Chem.* **1964**, *68*, 1322.

(22) Dorer, F. H.; Rabinovitch, B. S. *J. Phys. Chem.* **1965**, *69*, 1973.

(23) Holmes, B. E.; Paisley, S. D.; Rakestraw, D. J.; King, E. E. *Int. J. Chem. Kinet.* **1986**, *18*, 639.

(24) McDowell, D. R.; Weston, J.; Holmes, B. E. *Int. J. Chem. Kinet.* **1996**, *28*, 61.

(25) Williamson, A. D.; LeBreton, D. R.; Beauchamp, J. L. *J. Am. Chem. Soc.* **1976**, *98*, 2705.

(26) Seetula, J. A. *J. Chem. Soc., Faraday Trans.* **1998**, *94*, 1933.

(27) (a) Kerr, J. A.; Stocker, D. W. Standard Thermodynamics Properties of Chemical Substances. In *Handbook of Chemistry and Physics*; Lide, D. R., Jr., Ed.; CRC Press: Boca Raton, FL, 2002. (b) Bunker, P. R.; Sears, T. J. *J. Chem. Phys.* **1998**, *83*, 4866.

(28) Zachariah, M. R.; Westmoreland, P. R.; Burgess, D. R., Jr.; Tsang, W.; Melius, C. F. *J. Phys. Chem.* **1996**, *100*, 8737.

(29) Seetula, J. A. *J. Chem. Soc., Faraday Trans.* **1996**, *92*, 3070.

(30) Berkowitz, J.; Ellison, G. B.; Gutman, D. *J. Phys. Chem.* **1994**, *98*, 2744.

(31) (a) Yamada, T.; Lay, T. H.; Bozzelli, J. W. *J. Phys. Chem. A* **1998**, *102*, 7286. (b) Yamada, T.; Bozzelli, J. W. *J. Phys. Chem. A* **1999**, *103*, 7373. (c) Yamada, T.; Bozzelli, J. W.; Berry, R. J. *J. Phys. Chem. A* **1999**, *103*, 5602.

(32) Smith, D. W. *J. Phys. Chem. A* **1998**, *102*, 7086.

(33) Luo, Y. R.; Benson, S. W. *J. Phys. Chem. A* **1997**, *101*, 3042.

(34) Frisch, M. J.; Trucks, G. W.; Schlegel, H. B.; Scuseria, G. E.; Robb, M. A.; Cheeseman, J. R.; Montgomery, J. A., Jr.; Vreven, T.; Kudin, K. N.; Burant, J. C.; Millam, J. M.; Iyengar, S. S.; Tomasi, J.; Barone, V.; Mennucci, B.; Cossi, M.; Scalmani, G.; Rega, N.; Petersson, G. A.; Nakatsuji, H.; Hada, M.; Ehara, M.; Toyota, K.; Fukuda, R.; Hasegawa, J.; Ishida, M.; Nakajima, T.; Honda, Y.; Kitao, O.; Nakai, H.; Klene, M.; Li, X.; Knox, J. E.; Hratchian, H. P.; Cross, J. B.; Adamo, C.; Jaramillo, J.; Gomperts, R.; Stratmann, R. E.; Yazyev, O.; Austin, A. J.; Cammi, R.; Pomelli, C.; Ochterski, J. W.; Ayala, P. Y.; Morokuma, K.; Voth, G. A.; Salvador, P.; Dannenberg, J. J.; Zakrzewski, V. G.; Dapprich, S.; Daniels, A. D.; Strain, M. C.; Farkas, O.; Malick, D. K.; Rabuck, A. D.; Raghavachari, K.; Foresman, J. B.; Ortiz, J. V.; Cui, Q.; Baboul, A. G.; Clifford, S.; Cioslowski, J.; Stefanov, B. B.; Liu, G.; Liashenko, A.; Piskorz, P.; Komaromi, I.; Martin, R. L.; Fox, D. J.; Keith, T.; Al-Laham, M. A.; Peng, C. Y.; Nanayakkara, A.; Challacombe, M.; Gill, P. M. W.; Johnson, B.; Chen, W.; Wong, M. W.; Gonzalez, C.; Pople, J. A. *Gaussian 03*, revision B.04; Gaussian, Inc.: Pittsburgh, PA, 2003.

(35) (a) Pitzer, K. S.; Gwinn, W. D. *J. Chem. Phys.* **1942**, *10*, 428. (b) Pitzer, K. S. *J. Chem. Phys.* **1946**, *14*, 239.

(36) Keifer, J. H.; Katopodis, C.; Santhanam, S.; Srinivasan, N. K.; Tranter, R. S. *J. Phys. Chem. A* **2004**, *108*, 2443.

(37) (a) Dorfman, G.: Melchoir, A.; Rosenwaks, S.; Bar, I. *J. Phys. Chem. A* **2002**, *106*, 8285. (b) Melchoir, A.; Chen, X.; Bar, I.; Rosenwaks, S. *J. Chem. Phys.* **2000**, *112*, 10787.

(38) Stein, S. E.; Rabinovitch, B. S. *J. Chem. Phys.* **1972**, *58*, 2438.

(39) Guirgis, G. A.; Zhu, X.; Durig, J. R. *Struct. Chem.* **1999**, *10*, 445.

(40) Durig, J. R.; Godbey, S. E.; Sullivan, J. F. *J. Chem. Phys.* **1984**, *80*, 5983.

(41) Cadman, P.; Day, M.; Trotman-Dickenson, A. F. *J. Chem. Soc. A* **1970**, 2498.

(42) Cadman, P.; Day, M.; Trotman-Dickenson, A. F. *J. Chem. Soc. A* **1971**, 248.

(43) Guirgis, G. A.; Nanaie, H.; Durig, J. R. *J. Chem. Phys.* **1990**, *93*, 3837.

(44) Nanaie, H.; Guirgis, G. A.; Durig, J. R. *Spectrochim. Acta* **1993**, *49A*, 2039.

(45) Hartmann, H.; Bosche, H. G.; Heydtman, H. *Z. Phys. Chem.* **1964**, *42*, 329.

(46) (a) Durig, J. R.; Zhu, X.; Shen, S. *J. Mol. Struct.* **2001**, *570*, 1. (b) Luis, de Ana; Sang, M. E.; Lorenzo, F. J.; Lopez, J. C.; Alonso, J. C. *J. Mol. Spectrosc.* **1997**, *184*, 60.

(47) Kuramshina, G. M.; Pentin, Yu. A. *J. Mol. Struct.* **1999**, *480*−*481*, 161.

(48) Sun, L.; Hase, W. L. *J. Chem. Phys.* **2004**, *121*, 8831.

(49) Meerts, W. L.; Ozier, I. *Chem. Phys.* **1991**, *152*, 241.

(50) Hinze, R.; Lesarri, A.; López, J. C.; Alonso, J. L.; Guarnieri, A. *J. Chem. Phys.* **1996**, *104*, 9729.

(51) McGrath, M. P.; Rowland, F. S. *J. Phys. Chem. A* **2002**, *106*, 8191.

(52) (a) Heydtman, H.; Dill, B.; Jonas, R. *Int. J. Chem. Kinet.* **1975**, *7*, 973. (b) Jones, R.; Heydtman, H. *Ber. Bunsen-Ges. Phys. Chem.* **1978**, *82*, 823.

(53) Martell, J. M.; Kekenes-Huskey, P.; Holmes, B. E. Unpublished report, 2000.